

Temporal disorder does not forbid discontinuous absorbing phase transitions in low dimensional systems

M. M. de Oliveira¹ and C. E. Fiore²

¹*Departamento de Física e Matemática, CAP, Universidade Federal de São João del Rei, Ouro Branco-MG, 36420-000 Brazil,*

²*Instituto de Física, Universidade de São Paulo, São Paulo-SP, 05314-970, Brazil*

(Dated: September 11, 2021)

Recent papers have shown that spatial (quenched) disorder can suppress discontinuous absorbing phase transitions. Conversely, the scenario for temporal disorder is still unknown. In order to shed some light in this direction, we investigate its effect in three different two dimensional models which are known to exhibit discontinuous absorbing phase transitions. The temporal disorder is introduced by allowing the control parameter to be time dependent $p \rightarrow p(t)$, either varying as a uniform distribution with mean \bar{p} and variance σ or as a bimodal distribution, fluctuating between a value p and a value $p_l \ll p$. In contrast to spatial disorder, our numerical results strongly suggest that such uncorrelated temporal disorder does not forbid the existence of a discontinuous absorbing phase transition. We find that all cases are characterized by behaviors similar to their pure (without disorder) counterparts, including bistability around the coexistence point and common finite size scaling behavior with the inverse of the system volume, as recently proposed in Phys. Rev. E. **92**, 062126 (2015). We also observe that temporal disorder does not induce temporal Griffiths phases around discontinuous phase transitions, at least for $d = 2$.

PACS numbers: 05.70.Ln, 05.50.+q, 05.65.+bx

I. INTRODUCTION

Nonequilibrium phase transitions are considered a key feature of a countless number of phenomena, such as magnetic systems, biological and ecological models, water-like anomalies, and many others [1–4]. Recently, a considerable interest has been devoted to the inclusion of more realistic ingredients in order to describe (or mimic) the effects of impurities or external fluctuations, as well as their effects in the phase transition [5–10].

Commonly, these ingredients are introduced by allowing the control parameter to assume distinct values in space and/or time. The former case, regarded as quenched disorder, affects drastically the phase transitions, leading to the existence of a new universality classes and local regions in the absorbing phases, characterized by large activities with slow decays towards extinction. These rare regions typically arise when the activation rate λ lies between the clean value λ_c^0 (without disorder) and the dirty (disordered) critical point λ_c ; ie, $\lambda_c^0 < \lambda < \lambda_c$. Moreover, in these regions the system may exhibit non-universal exponents toward full extinction [11–13]. Heuristically, the Harris criterion [14] establishes that quenched disorder is a relevant perturbation if $d\nu_\perp < 2$, where d the system dimensionality and ν_\perp is the spatial correlation length exponent. For models belonging to the directed percolation (DP) universality class $\nu_\perp = 1.096854(4), 0.734(4)$ and $0.581(5)$ in $d = 1, 2$ and 3 , respectively. Consequently, the Harris criterion indicates that spatial disorder is a relevant perturbation for continuous absorbing phase transitions in all dimensions.

Conversely, the Imry-Ma [15] and Aizenman-Wehl [16] criteria establish that quenched disorder suppresses the phase coexistence in equilibrium systems for $d \leq 2$. Afterwards, it was shown [17–19] that the discontinuous

transition in the Ziff-Gulari-Barshad (ZGB) model becomes continuous when the disorder strength is large enough. More recently, Villa-Martín et al. [9] have suggested that the Imry-Ma-Aizenman-Wehl conjecture should be extended for discontinuous absorbing phase transitions for $d \leq 2$, irrespective of the disorder magnitude.

Although less studied than spatial disorder, the influence the temporal disorder has also been considered in some cases [20–22]. In contrast to the quenched disorder, here the control parameter becomes time-dependent, resulting in a temporarily active (ordered) as well as absorbing (disordered) phases, whose effect of variability becomes pronounced at the emergence of the phase transition. In particular, the available results have shown that temporal disorder is a highly relevant perturbation [23], suppressing the DP phase transitions in all dimension. For systems with up-down symmetry they are relevant only for $d \geq 3$. *Temporal Griffiths phases* (TGPs), a region in the active phase characterized by power-law spatial scaling and generic divergences of the susceptibility, have also been reported for absorbing phase transitions [21, 23–25], but not found in low dimensional systems with up-down symmetry [22]. On the other hand, the effect of temporal disorder for *discontinuous* absorbing phase transitions is still unknown.

In order to shed some light in this direction, here we investigate the effects of temporal disorder in discontinuous absorbing phase transition. Our study aims to answer three fundamental questions: (i) is the occurrence of phase coexistence forbidden under the presence of temporal disorder? (ii) if no, which changes does it provoke with respect to the pure (without disorder) version? (iii) Does the temporal disorder induce temporal Griffiths phases around these phase transitions? These ideas will be tested in three models which are known to

yield discontinuous absorbing phase transitions in two- and infinite-dimensional systems, namely the ZGB model for CO oxidation [26] and two lattice versions of the second Schlögl model (SSM) [12, 27]. As we will show, in all cases the phase transition is characterized by a behavior similar to their pure (without disorder) counterparts, including bistability around the coexistence point and common finite size scaling behavior with the inverse of the system volume, as recently proposed in [28].

This paper is organized as follows: In Sec. II we review the models studied and the simulation methods employed. Results and discussion are shown in Sec. III and conclusions are presented in Sec. IV.

II. MODELS AND METHODS

The SSM is single-species autocatalytic reaction model defined by the reactions $2A \rightarrow 3A$ and $A \rightarrow 0$, which occurs with transition rates 1 and α , respectively. Such system displays a discontinuous phase transition that can be qualitatively reproduced under a mean-field treatment. The first reaction predicts a particle growth following a quadratic dependence on the density, which makes low-density (active) state unstable and thus, a jump to a nonzero (large) density arises as the creation probability $1/(1 + \alpha)$ increases to a threshold value $\alpha_0 = 1/4$ [1]. Nonetheless, distinct works have claimed that these reaction rules are not sufficient to exhibit a discontinuity in a regular lattice [29]. In particular, the system dimensionality and the geometrical constraint of requiring the presence of a pair of adjacent particles surrounding an empty site (in order to fill the reaction $2A \rightarrow 3A$) are essential ingredients for the emergence of a phase coexistence [30, 31].

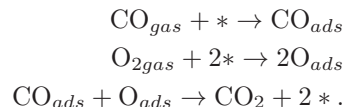
Here, we consider two square lattice versions of the SSM. The first one (SSM1), proposed by Windus and Jensen [32] and afterwards reconsidered in Ref. [9], is defined as follows: A given particle i is chosen (with equal probability) from a list of currently occupied sites and is annihilated with probability $p_a = \alpha/(1 + \alpha)$. Or, with probability $(1 - p_a)/4$, a nearest neighbor site of i , called site j , is also chosen at random. If the site j is empty, the particle i will diffuse for it. If j is filled by a particle, an offspring will be created at one of the neighboring sites of i and j (chosen with equal possibility) with probability p_b provided it is empty; otherwise nothing happens. The value $p_b = 0.5$ has been considered to directly compare our results with previous studies [9, 28, 32]. After above dynamics, the time is incremented by $1/N$, where N is the number of occupied sites.

For the second version, SSM2, the selection of particle i , its annihilation probability and the choice of the nearest neighbor site j are identical to SS1. However, in the SSM2 when a neighboring site j is chosen, its number of nearest neighbor occupied sites nn will be evaluated. A new offspring will be created at j with rate $nn/4$ provided $nn \geq 2$ and it is empty. More specifically, if $nn = 1$ no

particle will be created in the vacant site. On the contrary, if $nn = 2, 3$ or 4 , the creation will occur with probability $nn/4$.

It is worth mentioning that in the SSM1, the discontinuous transition is caused by both the diffusion and the creation of offsprings in the presence of two particles. Conversely, in the SSM2 model it is caused by the creation of offsprings in the presence of at least two species.

The third system we investigate is the ZGB model [26], which qualitatively reproduces some features of the oxidation of carbon monoxide on a catalytic surface. The surface is modeled as a square lattice, in which each site can be empty (*), or occupied by an oxygen (O_{ads}) or a carbon monoxide (CO_{ads}). It is summarized by the following reactions:



In practice, molecules of CO_{gas} and O_{2gas} hit the surface with complementary probabilities Y and $(1 - Y)$, respectively, at any time the chosen site is empty. At the surface, O_2 molecule dissociates into two independent O atoms, each one occupying two adjacent empty sites. If a $CO_{ads}O_{ads}$ pair is placed at neighboring sites on the surface, a CO_2 molecule will be formed, desorbing instantaneously and leaving both sites empty. As in the SSM models, after the above dynamics is implemented, time is incremented by $1/N$ where N is the total number of empty sites.

By changing the parameter Y , the model exhibits two phase transitions between an active steady state and one of two absorbing (“poisoned”) states, in which the surface is saturated either by O or by CO. The O-poisoned transition is found to be continuous. On the other hand, the CO-poisoned transition is discontinuous, and in this work we will focus on this specific case.

For the SSMs, the order parameter ϕ is the system density ρ and the transitions take place at $\alpha_0 = 0.0824(1)$ (SSM1) [28, 33] and $\alpha_0 = 0.2007(6)$ (SSM2) [34]. For the ZGB, ϕ is the density of CO and the transition occurs at $Y_0 = 0.5250(6)$ [28].

The temporal disorder is introduced so that at each time interval $t_i \leq t \leq t_i + \Delta t$, a generic control parameter p assumes a value extracted from a uniform distribution with mean \bar{p} and width σ . More specifically, p is evaluated using the formula $p = \bar{p} + (2\xi - 1)\sigma$, where ξ is a random number drawn at each time interval Δt from the standard uniform distribution in

$[0, 1]$. For the SSMs, \bar{p} corresponds to the creation probability $\bar{p} = 1 - p_a = \frac{1}{1 + \alpha}$, with a similar formula holding for the ZGB model with $1 - p_a$ replaced by Y .

In order to locate the transition point and the nature of the phase transition, we consider three alternative procedures. First, we follow the time behavior of the order-parameter $\phi(t)$, starting from a fully active initial configuration. In the active phase, it converges to a constant

value, signaling the permanent creation and annihilation of particles. On the other hand, $\phi(t)$ decays exponentially toward extinction (full poisoned state for the ZGB) in the absorbing phase. In the case of a typical (without disorder) continuous phase transitions, the above regimes are separated by a power-law decay $\phi(t) \sim t^{-\theta}$, with θ being the associated critical exponent. For the DP universality class, $\theta = 0.4505(10)$ in two dimensions [4]. In the presence of temporal disorder, the above critical behavior is replaced by $\phi(t) \sim (\ln t)^{-1}$ [24, 25]. Additionally, one does not expect similar behaviors at the emergence of a discontinuous transition.

The coexistence point can be estimated through a threshold value $\tilde{\alpha}$, which separates the saturation toward a definite value from an exponential decay [30, 35, 36]. Alternatively, a more reliable procedure is achieved by performing a finite-size analysis, as recently proposed in Ref. [28]. According to it, the difference between the pseudo-transition point α_L and the transition point α_0 scales with L^{-2} , where L^2 denotes the system volume (in two dimensions). The estimation of α_L can be done in a variety of ways. For instance, as corresponding to the peak of the system's order-parameter variance $\chi = L^2(\langle \phi^2 \rangle - \langle \phi \rangle^2)$, or even through the value in which the bimodal order parameter distribution presents two equal areas [28]. However, such scaling behavior is verified only by considering some kind of quasi-stationary (QS) ensemble, i.e. an ensemble of states accessed by the original dynamics at long times *conditioned on survival* (and restricted to those which are not trapped into an absorbing state). Here we employ an efficient numerical scheme given in Ref. [37], in which configurations are stored and gradually updated during the evolution of the stochastic process. Whenever the transition to the absorbing state is imminent, the system is “relocated” to a saved configuration. This accurately reproduces the results from the much longer procedure of performing averages only on samples that have not been trapped in the absorbing state at the end of their respective runs. The intensive quantities in a QS ensemble must converge to the stationary ones when $L \rightarrow \infty$.

Finally, in the third procedure, the mean survival time τ is considered for different system sizes. According to Refs. [9, 38], the coexistence point is the separatrix of an exponential growth of τ and an exponential increase until $L < L_c$ followed by a decreasing behavior for $L > L_c$. Here, we shall also quantify it, in order to compare with the pure (not disordered) cases.

III. RESULTS AND DISCUSSION

A. Models in a square lattice

The first analysis of the influence of temporal disorder is achieved by inspecting the time decay of the order parameter $\phi(t)$ starting from a fully active initial configuration for $t = 0$. For the SSM1, Figs. 1 and 2 (panels

(a)) show $\rho(t)$ for $\rho(0) = 1$ for the pure versions and for $\sigma = 0.05$ (not shown) and $\sigma = 0.15$, with $\Delta t = 1$.

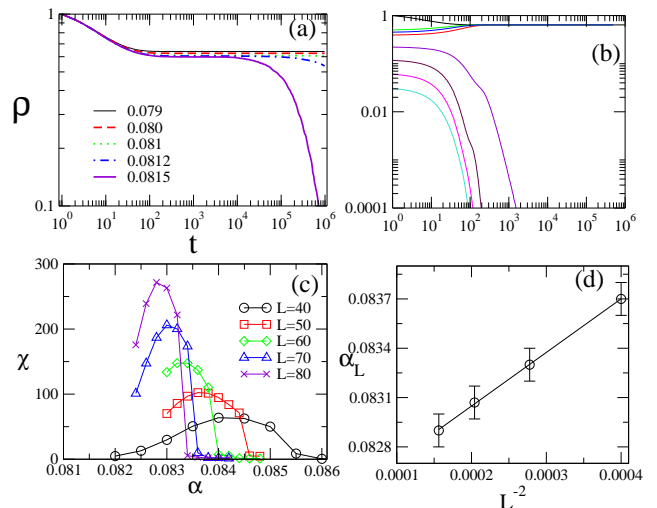


FIG. 1: (**Color online**): Results for the pure SSM1. Panel (a) shows the time decay of $\rho(t)$ for $\rho(0) = 1$ and distinct values of α . Panel (b) shows the bistable behavior of $\rho(t)$ close to the separatrix point $\tilde{\alpha} \sim 0.0815$ for distinct initial densities ranging from 10^{-2} to 1. Panel (c) and (d) show the order parameters variance χ versus α and the value α_L for which χ is maximum, vs $1/L^2$.

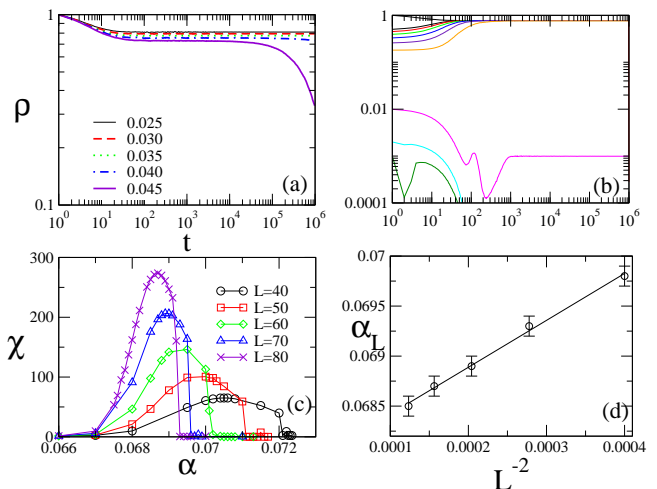


FIG. 2: (**Color online**): Results for $\sigma = 0.15$. Panel (a) shows the time decay of $\rho(t)$ for $\rho(0) = 1$ and distinct values of α . Panel (b) shows the bistable behavior of ρ at $\tilde{\alpha} \sim 0.035$ for distinct initial densities ranging from 10^{-2} to 1. Panel (c) and (d) show the order parameters variance χ versus α and the value α_L for which χ is maximum, vs $1/L^2$.

In all cases there is a threshold value $\tilde{\alpha}$ separating indefinite activity and exponential decay toward the particle extinction. They are strongly dependent on σ and occur at $\tilde{\alpha} = 0.0812, 0.076$ (not shown) and 0.035 for the pure, $\sigma = 0.05$ and 0.15 , respectively. No indication of a power-law have been verified nor a behavior of

type $\rho \sim (\ln t)^{-1}$. By repeating the above analysis for distinct initial configurations (panels (b)) with distinct densities ($10^{-2} \leq \rho(0) \leq 1$), the curves converge to two well defined stationary states, with $\rho \ll 1$ and $\rho \sim \rho^*$, signaling the bistability of active and absorbing phases, thus suggesting in all cases a first-order phase transition. For the pure, $\sigma = 0.05$ and 0.15 , ρ^* read $0.637(2)$, $0.63(2)$ and $0.77(2)$ respectively.

Inspection of quasi-stationary properties for distinct L 's reveal that the α_L 's (panels (c) and (d)), in which the order parameter variance χ is maximum, scales with $1/L^2$ and gives $\alpha_0 = 0.0824(2)$, $0.0823(2)$ (not shown) and $0.0680(2)$ for the pure, $\sigma = 0.05$ (not shown) and 0.15 , respectively. In particular for $L = 100$, the peak in χ occurs at $0.0827(1)$, $0.0826(1)$ and $0.0684(1)$, respectively. Therefore, both previous analyses suggest that temporal disorder does not forbid a discontinuous phase transition. However, it increases the metastable region at the emergence of the phase coexistence, i.e. $\alpha_L - \tilde{\alpha}$ increases with σ . This feature shares similarities with some procedures studied for characterizing the first-order transition in the ZGB and allied models close to the coexistence by taking different initial configurations [39].

An important point is that above the transition the number of points decrease substantially with increasing σ , revealing a suppression (absence) of a phase transition for $\sigma > 0.22$, which is a rather small disorder weight. In order to strengthen (i.e., to increase) the influence of disorder in the SSM1, we perform two changes. First we increase the disorder duration Δt . Since no larger values of σ are possible for this model, we change to a bimodal disorder distribution, where, at each Δt , the creation probability is chosen from two values, $p = 1/(1+\alpha)$ and $p_l = 1/(1+20\alpha)$, with rates $1-q$ and q , respectively. The results are presented in Fig. 3(a), (b) for $q = 0.2$, $L = 200$ and $\Delta t = 6$. Second, the analysis of the SSM2 for a larger value $\sigma = 0.4$ (with $\Delta t = 1$) is considered. Since its pure version yields a larger transition point, it is possible to increase substantially the value of σ (in contrast to the SSM1). These results are presented in Fig. 3 (panels (c) and (d)).

In both systems, the phase transitions obey the same pattern as the previous cases: separatrix points at $\tilde{\alpha} \sim 0.008$ ($\tilde{\alpha} \sim 0.005$) and bistable behaviors of $\rho(t)$ at the vicinity of the transition points [exemplified here for $\alpha = 0.007$ (and $\alpha = 0.001$)]. In both cases, the $\tilde{\alpha}$'s are very small, highlighting the relevance of disorder. As for the SSM1, the phase transition is suppressed for sufficiently large σ 's, whose results reveal the absence of a phase transition for $\sigma > 0.4$.

We now turn our attention to the ZGB model. In Figs. 4 and Fig. 5 we show the results for different disorder strengths, $\sigma = 0.05$ and $\sigma = 0.10$, respectively. In particular, we have considered rather small disorder strengths, in order not to "mix" both phase transitions. In both cases, results similar to the SSMs have been obtained. Panels (a) show once again the onset point \tilde{Y} separating activity from a exponential growth toward a full carbon

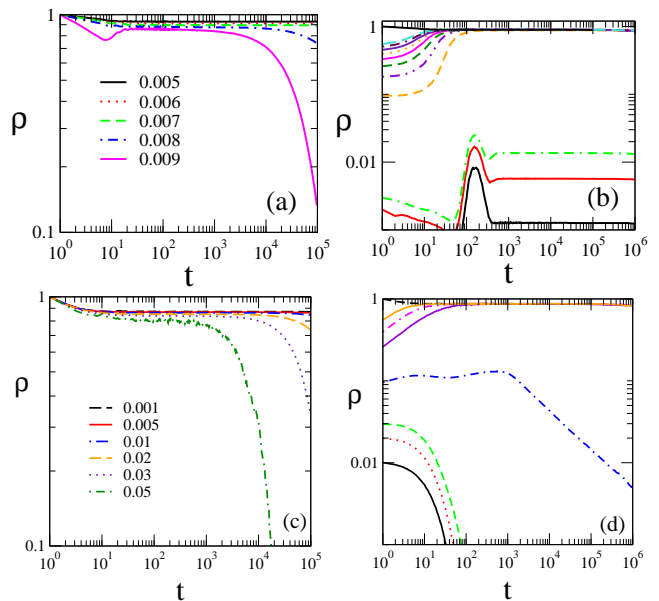


FIG. 3: (**Color online**) The SSM1 with bimodal temporal disorder distribution. (a) log-log time decay of ρ for distinct α 's and $\Delta t = 6$. (b) Bistable behavior of ρ at $\alpha = 0.007$ (very close to the separatrix point $\tilde{\alpha} \sim 0.008$) for distinct initial densities ranging from 10^{-3} to 1. Panel (c) shows the same analysis in (a), but for the SSM2 with uniform distribution for $\sigma = 0.4$ and $\Delta t = 1$. In (d), the bistable behavior of ρ at $\alpha = 0.001$, close to the transition point $\tilde{\alpha} \sim 0.005$, for distinct initial densities ranging from 10^{-3} to 1.

monoxide poisoning. The values of \tilde{Y} decrease by raising the disorder parameter σ , and read $\tilde{Y} = 0.527(1)$, $0.523(1)$, $0.516(1)$ and $0.500(2)$ for the pure, $\sigma = 0.05$, 0.1 and 0.2 (not shown), respectively. In addition, Y_L 's, obtained from the maximum of the order parameter variance χ scales with $1/L^2$ as seen in the pure version [28]. For the pure, $\sigma = 0.05$, 0.1 and 0.2 (not shown) we obtain $Y_0 = 0.5253(3)$, $0.524(1)$, $0.520(1)$ and $0.509(2)$, respectively. Although less pronounced than for the previous example, note that the difference $Y_0 - \tilde{Y}$ increases with σ , reinforcing that disorder increases the spinodal region around the phase coexistence.

Fig. 6 shows the mean lifetime of the QS state (defined as the time between two absorbing attempts during the QS regime), for the pure and disordered systems. We observe in all cases the same behavior (in similarity with Ref. [9]): a threshold value separating exponential growth of τ up to a maximum system size L_c , followed by a decrease of τ for $L > L_c$. For the pure cases, from such analysis the coexistence points are located within the interval $0.0805 < \alpha < 0.081$ (SSM1) and $0.5256 < Y < 0.5258$ (ZGB). In the presence of temporal disorder, they are in the interval $0.066 < \alpha < 0.067$ (SSM1 for $\sigma = 0.15$) and $0.515 < Y < 0.518$ (ZGB for $\sigma = 0.1$), which agrees with previous estimates obtained from the maxima of χ . Thus the above findings suggest that in contrast with critical transitions, τ does not grow

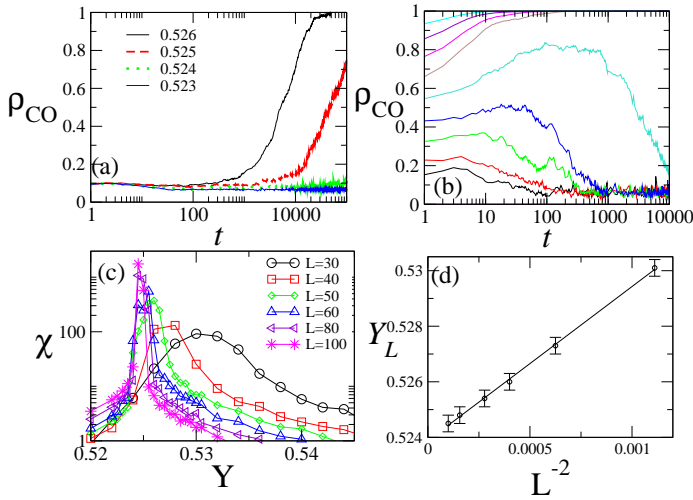


FIG. 4: (Color online): Results for the ZGB model for $\sigma = 0.05$. Panel (a) shows the time decay of ρ_{CO} for $\rho_{CO}(0) = 0$ and distinct values of Y . Panel (b) shows the bistable behavior of ρ_{CO} for $Y = 0.522$ for distinct initial densities equi-spaced in the interval $[0.1, 0.9]$ (Linear system size: $L = 800$). Panel (c) and (d) shows the order parameters variance χ versus Y and the Y_L , in which χ is maximum, vs $1/L^2$.

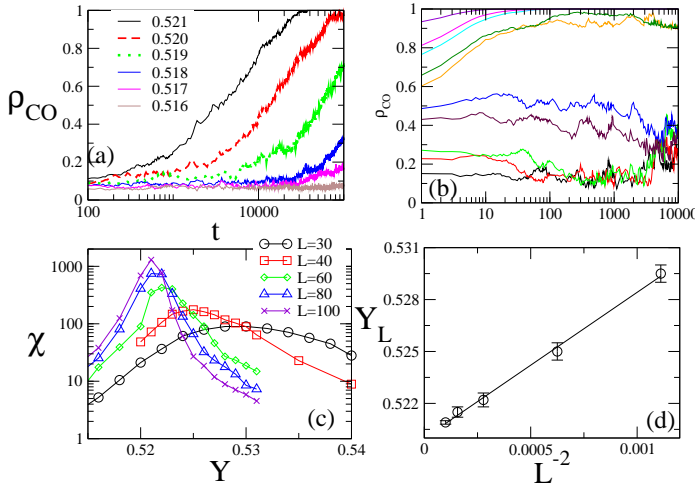


FIG. 5: (Color online): Results for the ZGB model for $\sigma = 0.10$. Panel (a) shows the time decay of ρ_{CO} for $\rho_{CO}(0) = 0$ and distinct values of Y . Panel (b) shows the bistable behavior of ρ_{CO} for $Y = 0.520$ for distinct initial densities equi-spaced in the interval $[0.1, 0.9]$ (Linear system size: $L = 800$). Panel (c) and (d) shows the order parameters variance χ versus Y and the Y_L , in which χ is maximum, vs $1/L^2$.

algebraically in a region within the active phase. These results are similar to those obtained for the generalized voter model [22], suggesting that TGP's do not manifest at discontinuous absorbing transitions, but only at critical ones [23–25]. However, this point still deserves further studies.

We close this section by remarking that the active-CO poisoned transition exhibits a behavior consistent to a

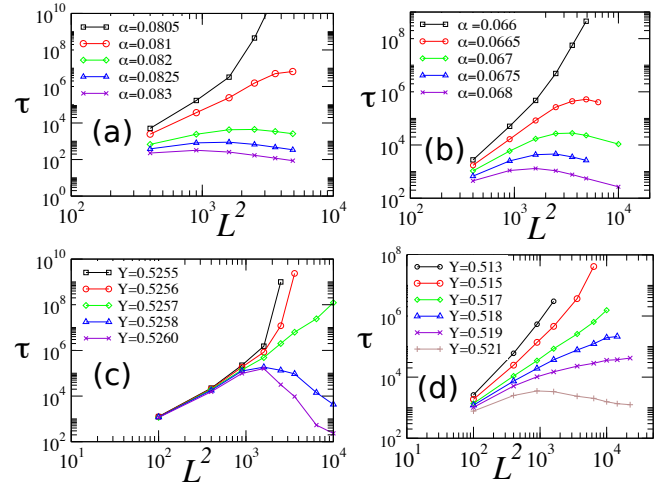


FIG. 6: (Color online): For the SSM1 (ZGB) model, panels (a)[(c)] and (b)[(d)] show the QS lifetime for the pure and disordered versions, respectively. We take $\sigma = 0.15$ and 0.1 for the SSM1 and ZGB models, respectively.

continuous transition for $\sigma > 0.3$ (not shown). Thus, in contrast to the SSMs (at least until $\sigma \leq 0.4$) numerical results indicate that the increase of σ suppress the phase coexistence.

B. Models in a complete graph

With the purpose of investigating the effects of temporal disorder in infinite-dimensional structures, the last analysis considers a mean-field like description of the above models, through a complete graph (CG) treatment. In the CG approach, each site interacts with all others, so that an exact analysis is allowed. For the SSM, besides the reactions $A \rightarrow 0$ and $2A \rightarrow 3A$, one takes the coagulation process $2A \rightarrow A$ occurring with rate ν [9, 40]. The discontinuous transitions yield at the exact points $\alpha_0 = 1/(2\sqrt{\nu})$ and $Y_0 = 2/3$ [40, 41], for the SSM and ZGB, respectively. Due to the prohibition against C–CO occupying nearest-neighbor pairs, only one species (CO or O) may be present at any moment for the ZGB analysis. Let $\rho = \rho_{CO} - \rho_O$ with ρ_{CO} and ρ_O denoting the fraction of sites bearing a CO and O, respectively. This quantity allows to describe a system of N sites completely by a single variable, with $\rho = -1$ representing the O-poisoned state and $\rho = 1$ the CO-poisoned state (see more details in Ref. [41]). In particular, we take $\nu = 1$ for the SSM and in all cases the temporal disorder was introduced in a similar fashion way than in Sec. II.

Our results for ρ for the SSM and ZGB models are shown in panels (a) of Figs. 7 and 8, respectively. In both cases, the analysis in the complete graph predicts behaviors which are similar to the numerical studies: the reduction of the active region, when compared to their pure counterparts and occurrence of bimodal probability distributions [see e.g panels (c)-(d) in Figs. 7 and 8]. In

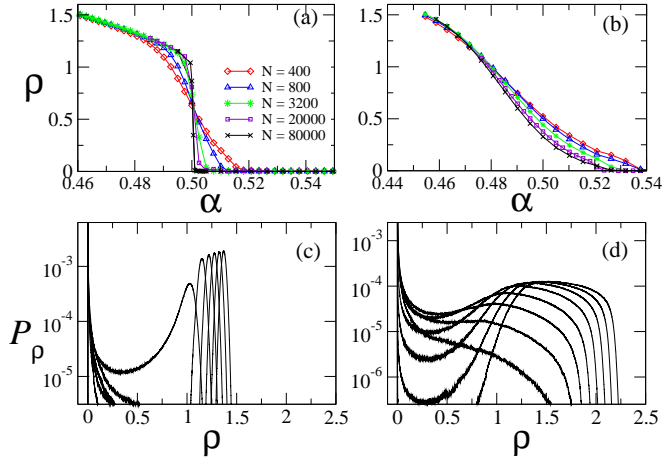


FIG. 7: (**Color online**): For the SSM on a complete graph, the QS density ρ for the pure model (a) and with temporal disorder strength $\sigma = 0.1$ (b). In (c), the QS probability distributions for the pure model, with α ranging from 0.475 to 0.525. In (d), the same as (c) but for $\sigma = 0.1$, and α ranging from 0.4750 to 0.5625. System size: $N = 10000$ in (c) and (d).

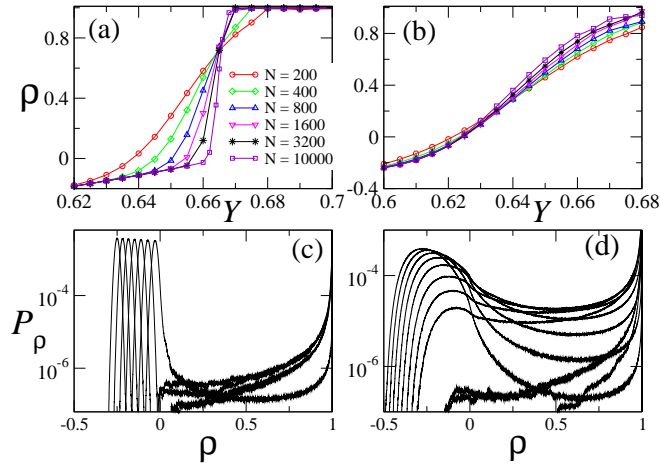


FIG. 8: (**Color online**): For the ZGB model on a complete graph, the QS order-parameter ρ for the pure model (a) and with temporal disorder strength $\sigma = 0.1$ (b). In (c), the QS probability distributions for the pure model, with Y ranging from 0.60 to 0.70. In (d), the same as (c) but for $\sigma = 0.1$, and Y ranging from 0.60 to 0.70. System size: $N = 10000$ in panels (c) and (d).

particular, for disorder strength $\sigma = 0.1$, the transition points are shifted from $\alpha_0 = 0.5$ to $\alpha_0 = 0.526$ (SSM), and from $Y_0 = 2/3$ to $Y_0 = 0.635$ (ZGB). Thus, the inclusion of low disorder maintains the phase coexistence. However, by increasing σ the active phase peaks become broader, suggesting the appearance of a continuous transition as shown in Fig. 9 (a) and (b). Despite this, there are some differences when compared to their low dimensional counterparts. There is a region in the active phase (see e.g Fig. 9 (c) and (d)), in which τ grows slower than

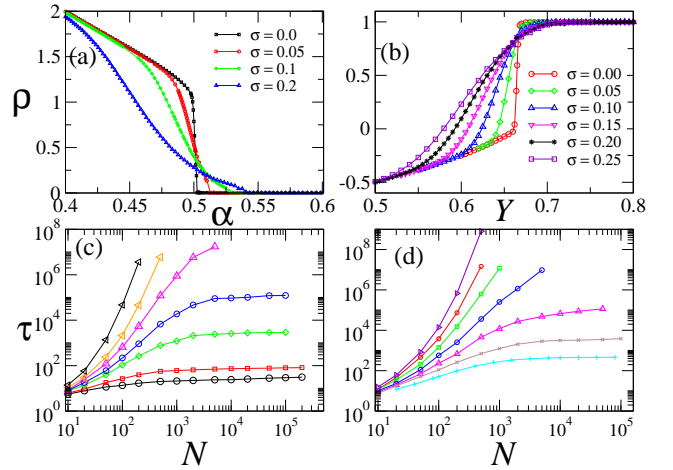


FIG. 9: (**Color online**): For the complete graph, panels (a) and (b) show the QS order-parameter ρ for the SSM and ZGB models, respectively for distinct σ 's and $N = 10000$. Panel (c) shows τ versus N for the SSM model on a complete graph for $\sigma = 0.1$ and α ranging from $\alpha = 0.458, 0.467, 0.472, 0.476, 0.481, 0.490$, and 0.500 (from top to bottom). In (d), the same in (c) but for the ZGB with $\sigma = 0.1$ and Y ranging from 0.55 to 0.61 (equi-spaced from top to bottom).

exponential, and then it saturates at a finite value. This behavior is related to the abrupt transition that occurs when the noise takes the control parameter to a value that drives the system to the absorbing state. Since configurations with intermediary densities are unstable in these systems, one observes a bimodal QS probability distribution in this region. This behavior is remarkably distinct from TGP, in which τ increases algebraically with the system size L and it has been observed only in continuous (absorbing) phase transitions.

IV. CONCLUSIONS

We studied the influence of temporal disorder in the context of discontinuous absorbing phase transitions. We investigated extensively three models by means of distinct numerical procedures. Our results strongly suggest that in contrast to the spatial disorder, discontinuous absorbing transitions are not forbidden by the presence of temporal disorder in low dimensional systems. In particular, the behavior of quantities are similar to their pure counterparts. However, the temporal disorder increases the metastable region close to phase coexistence.

Our results also suggest the absence of temporal Griffiths phases (TGPs). Some remarks over their existence are in order: Earlier results for different systems have shown that the inclusion of temporal disorder does not necessarily lead to the presence of TGPs [22]. Although it suppresses the DP universality class in all dimensions, the appearance of TGPs depend on σ and/or Δt [24, 25]. Similar conclusions continue to be valid for distinct up-

down systems, in which only for $d \geq 3$ TGP are observed. Recent results for a one-dimensional example [42] confirm the absence of TGPs when the phase transition is discontinuous.

For the complete graph versions ($d \rightarrow \infty$), we observe the maintenance of the phase coexistence for small disorder. However, in contrast to the lattice versions, there is a region in the active phase in which the lifetime grows slower than exponential and then saturate at a finite value.

It is worth emphasizing that our results do not exclude a discontinuous transition becoming continuous from a disorder threshold σ_c . Except for the SSMS, in which the transition points decrease substantially as σ increases, results for the ZGB model indicate the suppression of phase coexistence for $\sigma > 0.3$. Again, the CG approach and the above mentioned one-dimensional case also reveal similar trends. This last case shows that the crossover to the criticality is also followed by appearance of TGPs within the active phase [42].

Possible extensions of this work include the study of

the effect of temporal correlated disorder and the more general case of spatio-temporal disorder, i.e. how the discontinuous phase transition is affected by an external perturbation that fluctuates in both space and time [43]. Both cases appear to be of particular interest in the context of ecosystems, where the effects of noise on the extinction of a population due to environmental changes have been attracting considerable attention recently [44]. Also, extension of both models for larger dimensions are intended to be investigated, in order to confirm the above hypotheses.

ACKNOWLEDGMENT

We acknowledge Gabriel T. Landi and J. A. Hoyos for fruitful discussions. The financial supports from CNPq and FAPESP, under grants 15/04451-2 and 307620/2015-8, are also acknowledged.

-
- [1] J. Marro and R. Dickman, *Nonequilibrium Phase Transitions in Lattice Models* (Cambridge University Press, Cambridge, 1999).
- [2] H. Hinrichsen, *Adv. Phys.* **49**, 815 (2000).
- [3] G. Ódor, *Rev. Mod. Phys.* **76**, 663 (2004).
- [4] M. Henkel, H. Hinrichsen and S. Lubeck, *Nonequilibrium Phase Transitions Volume I: Absorbing Phase Transitions* (Springer-Verlag, The Netherlands, 2008).
- [5] G. M. Buendia and P. A. Rikvold, *Phys. Rev. E* **88**, 012132 (2013).
- [6] V. Bustos, R. O. U nac, and G. Zgrablich, *Phys. Rev. E* **62**, 8768 (2000).
- [7] D.-J. Liu, X. Guo, and J. W. Evans, *Phys. Rev. Lett.* **98**, 050601 (2007).
- [8] C. Buono, F. Vazquez, P. A. Macri, and L. A. Braunstein *Phys. Rev. E* **88**, 022813 (2013).
- [9] P. Villa Martín, J. A. Bonachela and M. A. Muñoz, *Phys. Rev. E* **89**, 012145 (2014).
- [10] M. M. de Oliveira, S. G. Alves and S. C. Ferreira, *Phys. Rev. E* **93**, 012110 (2016).
- [11] J. Hooyberghs, F. Igloi, and C. Vanderzande, *Phys. Rev. Lett.* **90**, 100601 (2003).
- [12] M. M. de Oliveira and S. C. Ferreira, *J. Stat. Mech.* **2008**, P11001 (2008).
- [13] See for example, T. Vojta and M. Dickison, *Phys. Rev. E* **72**, 036126 (2005); H. Barghathi and T. Vojta, *Phys. Rev. Lett* **109**, 170603 (2012).
- [14] A. B. Harris, *J. Phys. C* **7**, 1671 (1974).
- [15] Y. Imry and S.-k. Ma, *Phys. Rev. Lett.* **35**, 1399 (1975).
- [16] M. Aizenman and J. Wehr, *Phys. Rev. Lett.* **62**, 2503 (1989).
- [17] J.-P. Hovi, J. Vaari, H.-P. Kaukonen, and R.M. Nieminen, *Comput. Mater. Sci.* **1**, 33 (1992).
- [18] J. Cortés and E. Valencia, *Surf. Sci.* **425**, L357 (1999).
- [19] G. L. Hoenicke and W. Figueiredo, *Phys. Rev. E* **62**, 6216 (2000).
- [20] I. Jensen, *Phys. Rev. Lett.* **77**, 4988 (1996).
- [21] F. Vazquez, J. A. Bonachela, C. López and M. A. Muñoz, *Phys. Rev. Lett.* **106**, 235702 (2011).
- [22] R. Martínez-García, F. Vazquez, C. López, and M. A. Muñoz, *Phys. Rev. E* **85**, 051125 (2012).
- [23] J. A. Hoyos and T. Vojta, *Europhysics Lett.* **112**, 30002 (2015).
- [24] H. Barghathi, T. Vojta and J. A. Hoyos, *Phys. Rev. E* **94**, 022111 (2016).
- [25] C. M. D. Solano, M. M. de Oliveira and C. E. Fiore, *Phys. Rev. E*, accepted (2016). arXiv:1609.05841.
- [26] R. M. Ziff, E. Gulari, and Y. Barshad, *Phys. Rev. Lett.* **56**, 2553 (1986).
- [27] F. Schlögl, *Z. Phys.* **253**, 147 (1972).
- [28] M. M. de Oliveira, M. G. E. da Luz and C. E. Fiore *Phys. Rev. E* **92**, 062126 (2015).
- [29] See e.g. C. Varghese and R. Durrett, *Phys. Rev. E* **87**, 062819 (2013).
- [30] C. E. Fiore, *Phys. Rev. E* **89**, 022104 (2014).
- [31] As exemplified in distinct examples in [30], whenever the $2A \rightarrow 3A$ is replaced by $A \rightarrow 2A$, the transition becomes continuous.
- [32] A. Windus and H. J. Jensen, *J. Phys. A* **40**, 2287 (2007).
- [33] In fact, our estimate is different to the estimate $\alpha_c = 0.0742(1)$ [28], as a result of a slightly different dynamics implementation.
- [34] E. F. da Silva and M. J. de Oliveira, *Comp. Phys. Comm.* **183**, 2001 (2012).
- [35] S. Pianegonda and C. E. Fiore, *J. Stat. Mech.* 2015, P08018 (2015).
- [36] S. Pianegonda and C. E. Fiore, *Physica A* **451**, 349 (2016).
- [37] M. M. de Oliveira and R. Dickman, *Phys. Rev. E* **71**, 016129 (2005); *Braz. J. Phys.* **36**, 685 (2006).
- [38] S. Tanase-Nicola and D. K. Lubensky, *Phys. Rev. E* **86**, 040103 (2012).

- [39] J. W. Evans and M. S. Miesch, Surf. Sci. **245**, 401 (1991).
- [40] R. Dickman and R. Vidigal, J. Phys. A **35**, 1147 (2002).
- [41] M. M. de Oliveira and R. Dickman, Physica A **343**, 525 (2004).
- [42] C. E. Fiore and M. M. de Oliveira (in progress).
- [43] T. Vojta and R. Dickman, Phys. Rev. E. **93**, 032143 (2016).
- [44] O. Ovaskainen and B. Meerson, Trends in Ecology & Evolution **25**, 643 (2010).